# Jet measurements in CMS

**Daniel Savoiu** on behalf of the CMS Collaboration

*LP2021, Manchester, 12 January 2022*

# Jets at hadron colliders

## Direct measurements

- determination of **fundamental QCD parameters ($\alpha_s$)** and **PDFs**
- jets produced in large numbers
  → high **statistical precision**

precision **measurements**
*LHC*: **jet cross sections** at $\sqrt{s}$ = 13 TeV

fixed-order **theory**
*state of the art*: **NNLO pQCD**

Fit

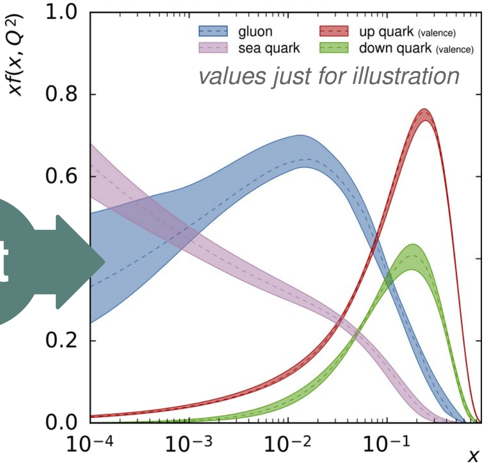


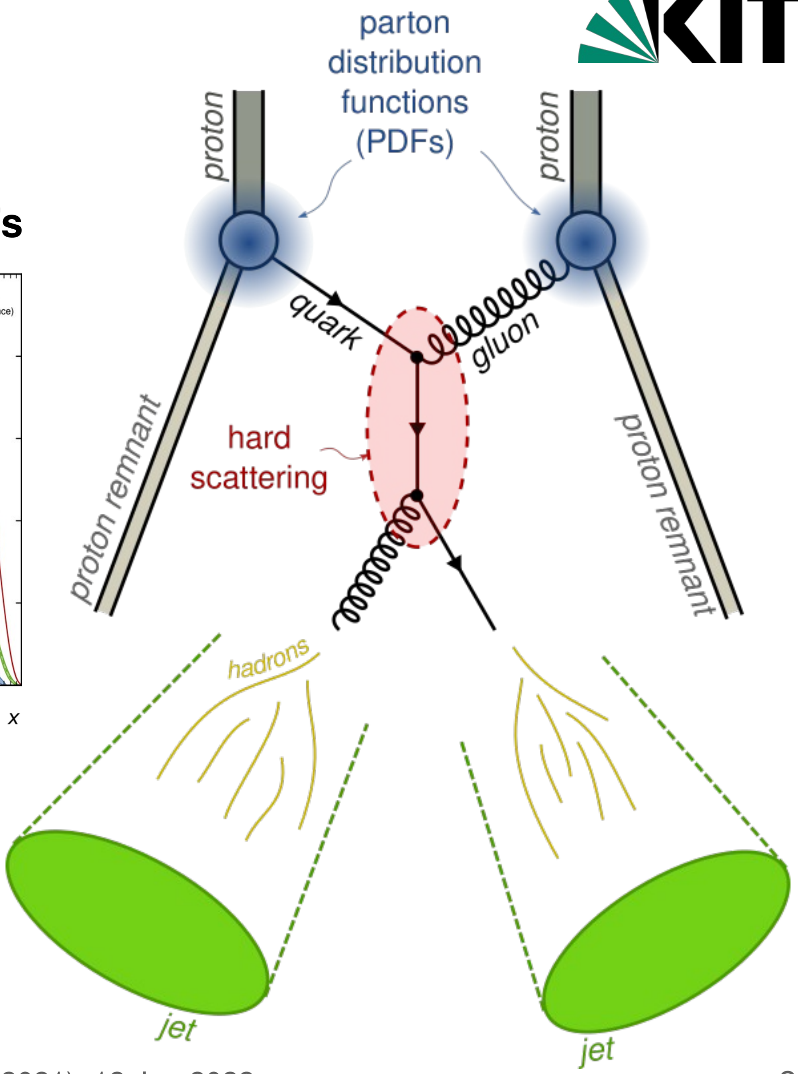


## Insights beyond pure QCD

- exploit precision of jet observables to probe rare processes, or to constrain extensions to the Standard Model
- improve experimental methods (pileup, reconstruction, resolution effects) & theoretical models (parton shower, underlying event, hadronization, MPI)

# Inclusive jet production at $\sqrt{s}$ = 13 TeV

[1] **CMS-SMP-20-011**
arXiv:2111.10431

double-differential cross section in jet $p_T$ and rapidity $y$

anti-$k_T$ jets with $R = 0.4$ and 0.7 (shown here: $R = 0.7$)

comparison to pQCD theory at NLO+NLL and NNLO
+ non-perturbative (NP) and electroweak (EW) corrections

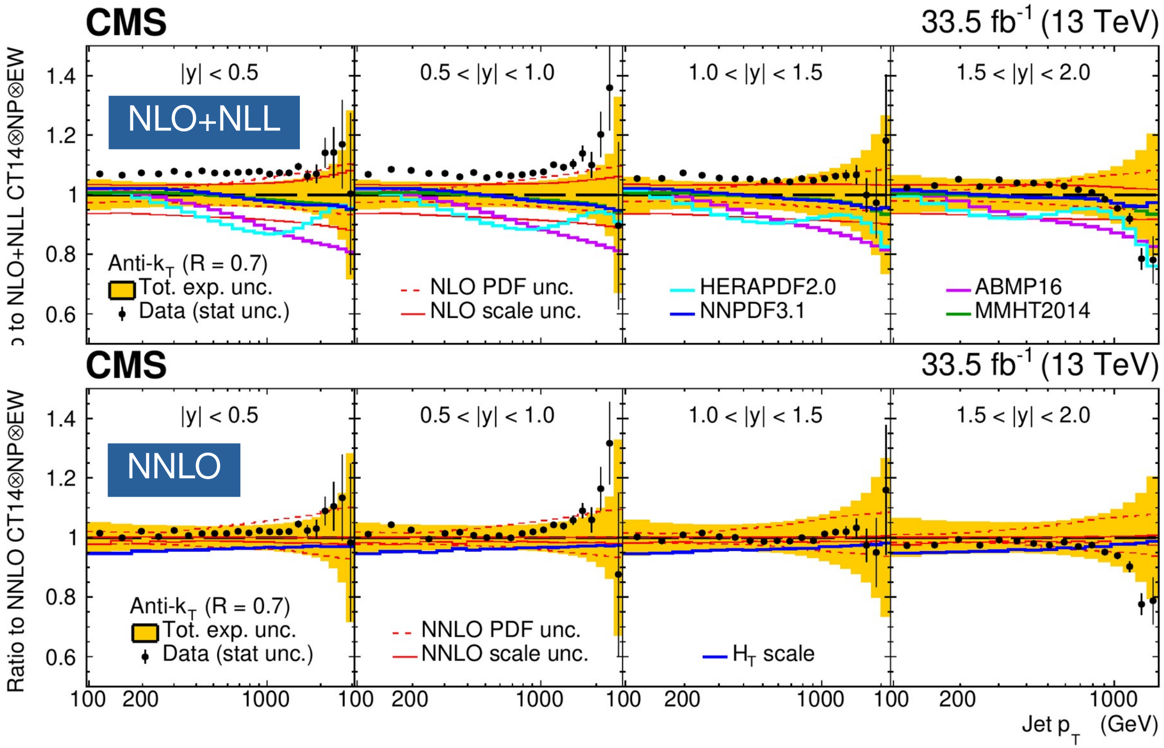


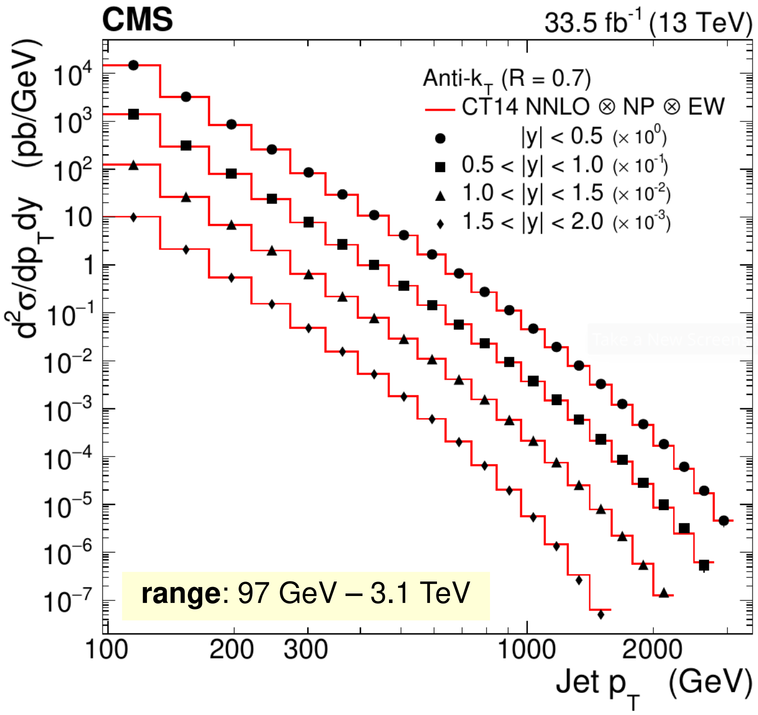


overall good description of data by theory, tangible improvement at NNLO

*however*, predictions differ between PDFs, theory uncertainties remain large

# Inclusive jet production at $\sqrt{s}$ = 13 TeV

[1] **CMS-SMP-20-011**
arXiv:2111.10431

## PDF + $\alpha_s(m_Z)$ fit at NNLO

determine PDFs and QCD parameters in a fit to the present CMS jet data together with data from HERA and using a HERAPDF-like PDF parametrization

$$x\,g(x) = A_g\, x^{B_g}\,(1-x)^{C_g}\,(1 + D_g x + E_g x^2)$$
$$x\,u(x) = A_u\, x^{B_u}\,(1-x)^{C_u}\,(1 + E_u x^2)$$
$$x\,d(x) = A_d\, x^{B_d}\,(1-x)^{C_d}$$
$$x\,\bar{U}(x) = A_{\bar{U}}\, x^{B_{\bar{U}}}\,(1-x)^{C_{\bar{U}}}\,(1 + D_{\bar{U}} x)$$
$$x\,\bar{D}(x) = A_{\bar{D}}\, x^{B_{\bar{D}}}\,(1-x)^{C_{\bar{D}}}\,(1 + E_{\bar{U}} x^2)$$

**strong coupling** in good agreement with world average and previous CMS results

$\alpha_s(m_Z)$ = **0.1170** ± 0.0014 (fit)
± 0.0007 (model)
± 0.0008 (scale)
± 0.0001 (parametrization)

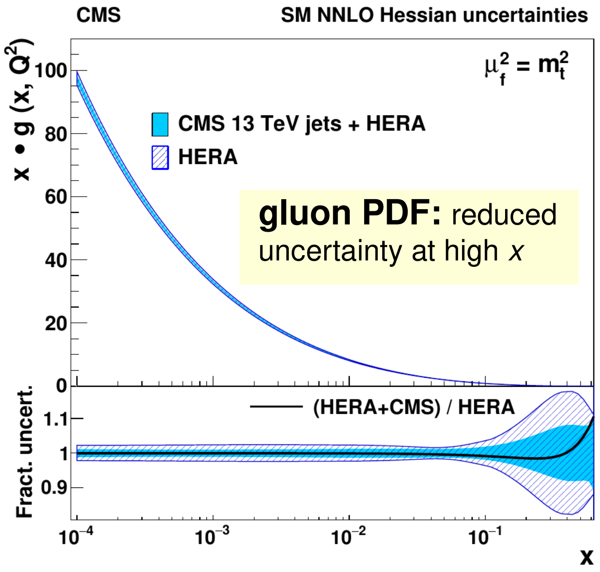


**gluon PDF:** reduced uncertainty at high $x$

| Data sets | | HERA-only Partial $\chi^2/N_{dp}$ | HERA+CMS Partial $\chi^2/N_{dp}$ |
|---|---|---|---|
| HERA I+II neutral current | $e^+p$, $E_p$ = 920 GeV | 378/332 | 375/332 |
| HERA I+II neutral current | $e^+p$, $E_p$ = 820 GeV | 60/63 | 60/63 |
| HERA I+II neutral current | $e^+p$, $E_p$ = 575 GeV | 201/234 | 201/234 |
| HERA I+II neutral current | $e^+p$, $E_p$ = 460 GeV | 208/187 | 209/187 |
| HERA I+II neutral current | $e^-p$, $E_p$ = 920 GeV | 223/159 | 227/159 |
| HERA I+II charged current | $e^+p$, $E_p$ = 920 GeV | 46/39 | 46/39 |
| HERA I+II charged current | $e^-p$, $E_p$ = 920 GeV | 55/42 | 56/42 |
| CMS inclusive jets 13 TeV | $0.0 < \lvert y\rvert < 0.5$ | — | 13/22 |
| | $0.5 < \lvert y\rvert < 1.0$ | — | 31/21 |
| | $1.0 < \lvert y\rvert < 1.5$ | — | 18/19 |
| | $1.5 < \lvert y\rvert < 2.0$ | — | 14/16 |
| Correlated $\chi^2$ | | 66 | 83 |
| Global $\chi^2/N_{dof}$ | | 1231/1043 | 1321/1118 |

**good fit quality**
→ $\chi^2/N_{dof}$ ~ 1.18

# Inclusive jet production at $\sqrt{s}$ = 13 TeV

[1] **CMS-SMP-20-011**
arXiv:2111.10431

PDF + $\alpha_s(m_Z)$ + $m_t^{\,(\mathrm{pole})}$ fit at NLO

fit inclusive jet and $t\bar{t}$ data simultaneously to benefit from constraining power of inclusive jet data on PDFs & strong coupling constant

constrain EFT extensions to the Standard Model involving four-quark contact interactions (CI)

**top quark mass** in good agreement with previous CMS results using only $t\bar{t}$ data

$m_t^{\,(\mathrm{pole})}$ [GeV] = **170.4** ± 0.6 (fit) ± 0.1 (model) ± 0.1 (scale) ± 0.1 (parametrization)

**strong coupling** in good agreement with world average and previous CMS results

$\alpha_s(m_Z)$ = **0.1188** ± 0.0017 (fit) ± 0.0004 (model) ± 0.0025 (scale) ± 0.0001 (parametrization)

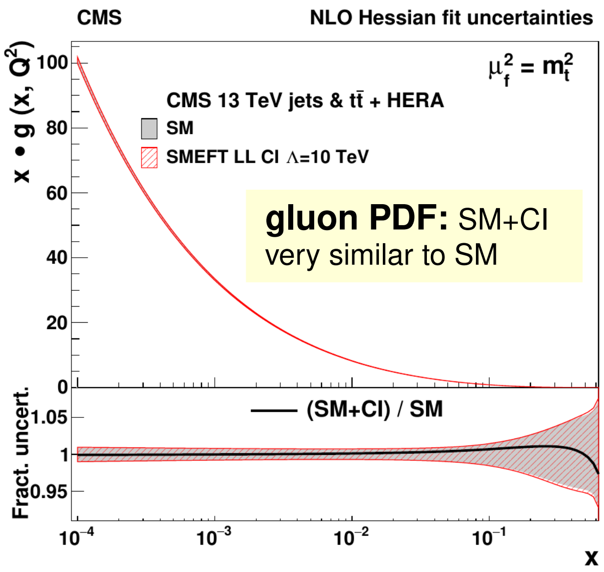


**gluon PDF:** SM+CI very similar to SM

**constraints on CI model** → fit *Wilson coefficient* $c_1$ as free parameter, no significant deviation from SM expectation ($c_1$ = 0)

$$\mathcal{L}_{\mathrm{SMEFT}} = \mathcal{L}_{\mathrm{SM}} + \frac{2\pi}{\Lambda^2} \sum_{n\in\{1,3,5\}} c_n O_n$$

**energy scale Λ of the new CI**

→ investigated range from 5 to 50 TeV

→ exclusion limit on CI model: Λ > 24 TeV (95% CL for left-handed CI with $c_1$ = –1)

**CI couplings** → three scenarios, fix relationship between Wilson coefficients:

**axial** → $c_3 = -2c_1$, $c_5 = c_1$
**vector** → $c_3 = 2c_1$, $c_5 = c_1$
**left-handed** → $c_3 = c_5 = 0$

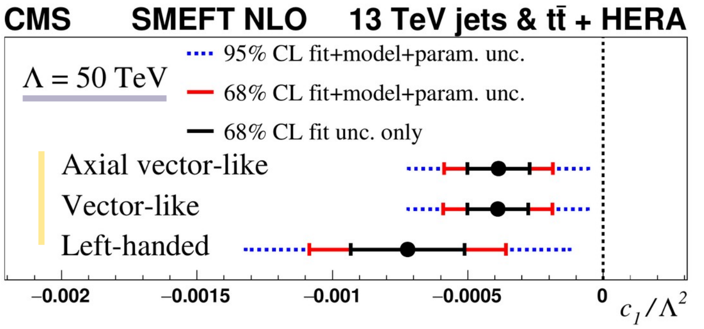

# Inclusive jet production at $\sqrt{s}$ = 5.02 TeV

[2] **CMS-SMP-21-009**

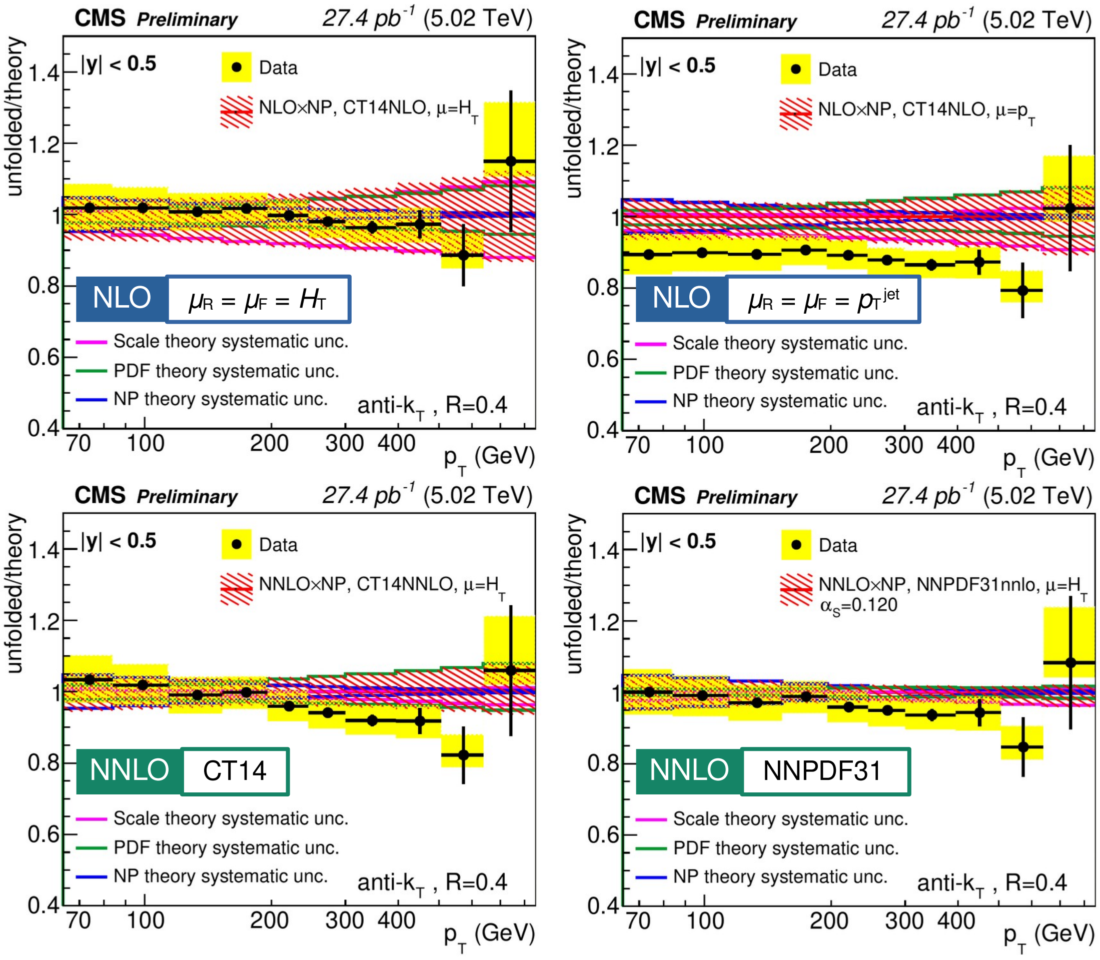


complementary measurement at lower center-of-mass energy using anti-$k_T$ jets with $R = 0.4$

study of data/theory agreement at NLO and NNLO for different PDF sets and central scale choices for $\mu_R$ & $\mu_F$

**sensitivity to strong coupling constant**
among NNLO predictions obtained with NNPDF31nnlo PDFs closest agreement with data observed for ***$\alpha_s(m_Z)$ = 0.120***

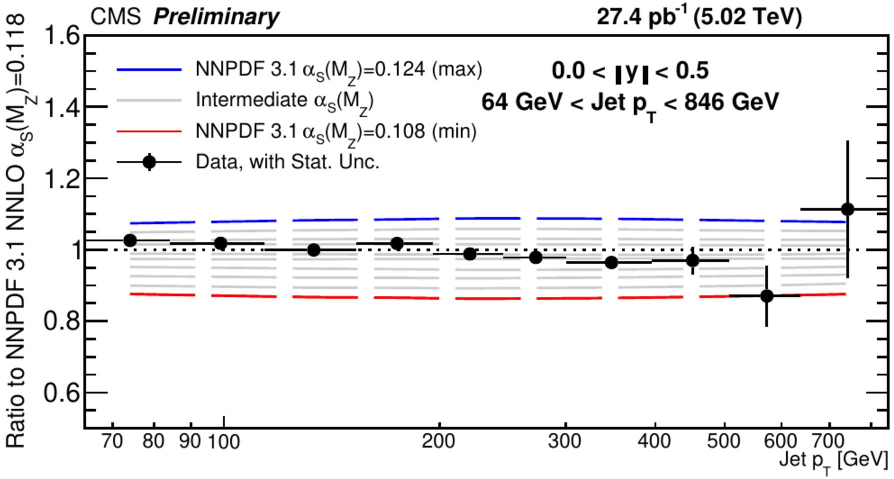

# Multijet measurements

[3] **CMS-SMP-21-006**

## $p_T$ spectra of first four $p_T$-leading jets are measured in multijet events

benchmark for SM calculations, in particular parton showers for higher jet multiplicities

conventional parton shower + collinear PDFs are compared to newer models using parton branching (PB) approach with transverse-momentum-dependent PDFs (TMDs)

[5, 6]

Table 1: Description of the simulated samples used in the analysis.

| generator | PDF | matrix element | tune |
|---|---|---|---|
| PYTHIA 8 [21] | NNPDF 2.3 (LO) | LO $2 \to 2$ | CUETP8M1 |
| MADGRAPH+PY8 [4] | NNPDF 2.3 (LO) | LO $2 \to 2, 3, 4$ | CUETP8M1 |
| HERWIG++ [24] | CTEQ6L1 (LO) | LO $2 \to 2$ | CUETHppS1 |
| MG5_AMC+PY8 (*jj*) | NNPDF 3.0 (NLO) | NLO $2 \to 2$ | CUETP8M1 |
| MG5_AMC+CA3 (*jj*) | PB set 2 (NLO) | NLO $2 \to 2$ | – |
| MG5_AMC+CA3 (*jjj*) | PB set 2 (NLO) | NLO $2 \to 3$ | – |

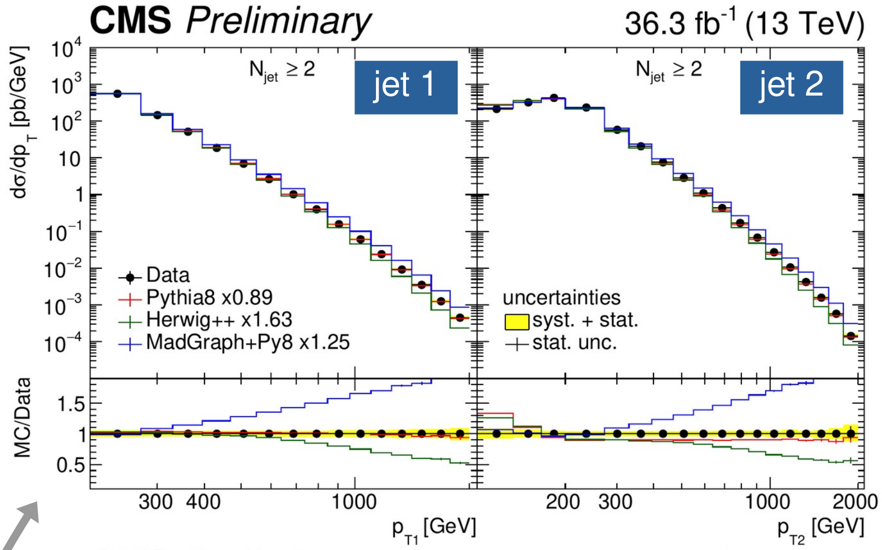


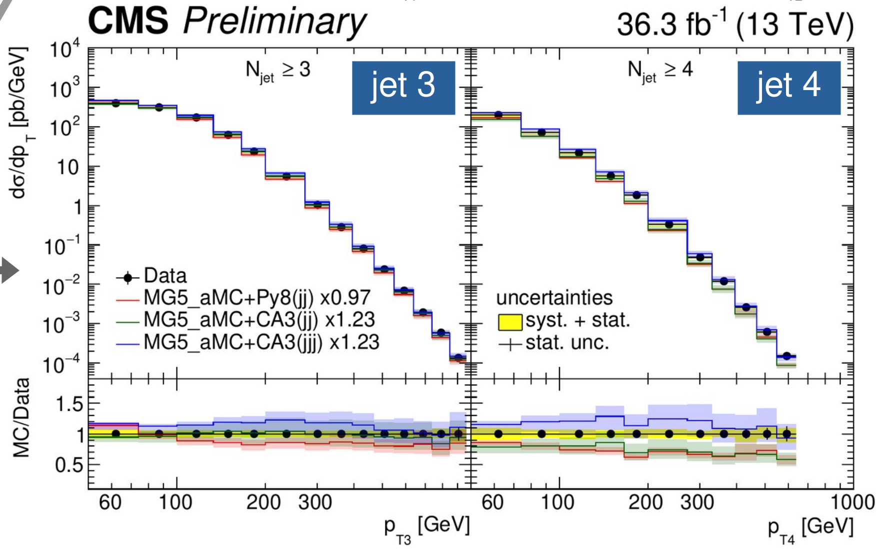


disagreement between LO models at high $p_T$, NLO models perform better

conventional and PB-TMD approaches yield comparable results

# Multijet measurements [3]

jet multiplicity in bins of leading jet $p_T$ and azimuthal angle separation $\Delta\phi_{1,2}$

can measure multiplicities of up to seven jets

conventional parton shower + collinear PDFs
vs. parton branching (PB) approach + TMDs [5, 6]

Table 1: Description of the simulated samples used in the analysis.

| generator | PDF | matrix element |
|---|---|---|
| PYTHIA 8 [21] | NNPDF 2.3 (LO) | LO $2 \to 2$ |
| MADGRAPH+PY8 [4] | NNPDF 2.3 (LO) | LO $2 \to 2, 3, 4$ |
| HERWIG++ [24] | CTEQ6L1 (LO) | LO $2 \to 2$ |
| MG5_AMC+PY8 (*jj*) | NNPDF 3.0 (NLO) | NLO $2 \to 2$ |
| MG5_AMC+CA3 (*jj*) | PB set 2 (NLO) | NLO $2 \to 2$ |
| MG5_AMC+CA3 (*jjj*) | PB set 2 (NLO) | NLO $2 \to 3$ |

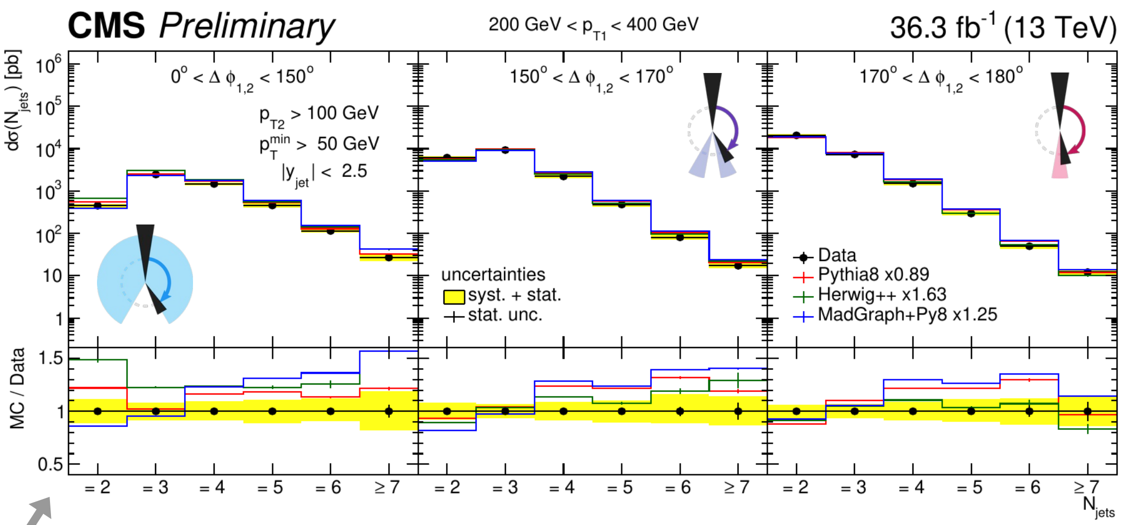


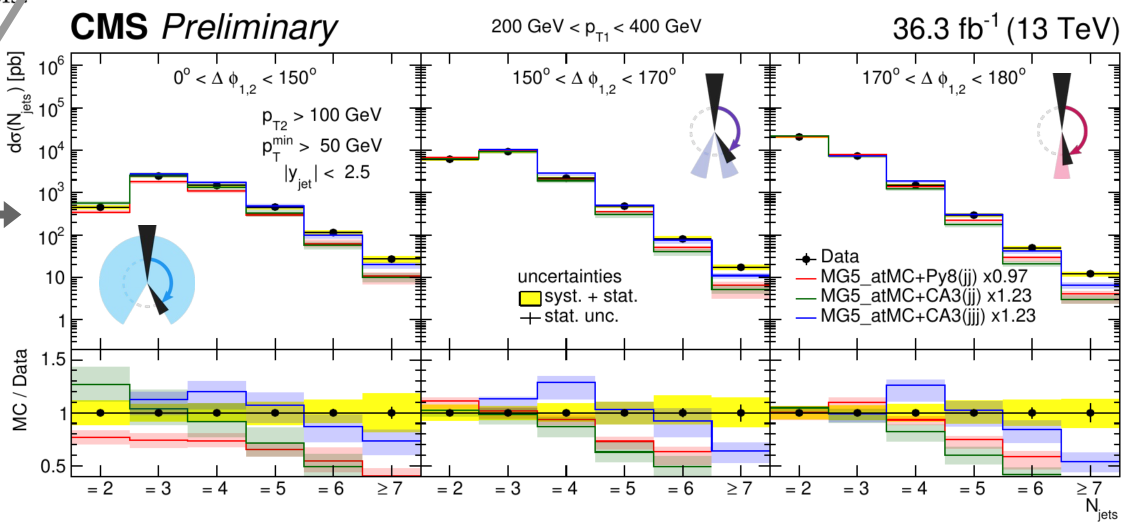


overall reasonable description by LO models

NLO models mostly describe the low-multiplicity region, but perform worse at higher multiplicities

# Jet substructure measurements

[4] **CMS-SMP-20-010**
arXiv:2109.03340

useful tool for distinguishing between quark and gluon jets
and evaluating the performance of MC simulations

**dijet** (*gluon-jet-enriched*) vs.
**Z+Jet** (*quark-jet-enriched*)

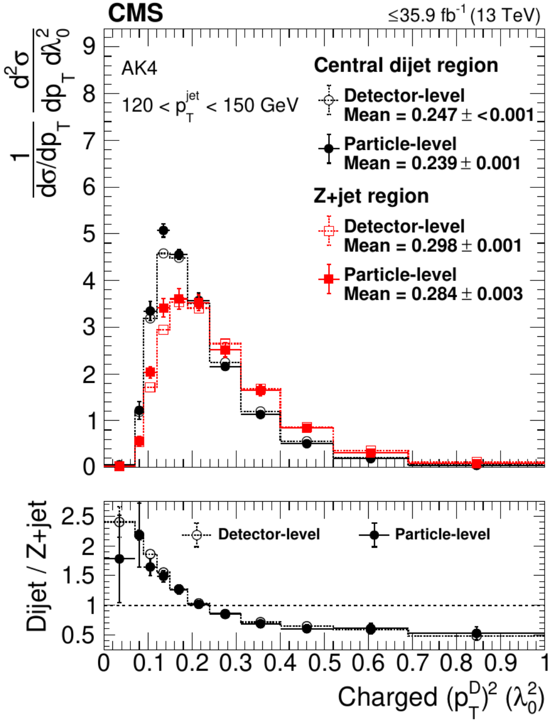


**large number of measurements** performed

| Dimension | | Variants |
|---|---|---|
| Region | × 3 | Z+jet vs. central dijet vs. forward dijet |
| Observable $\lambda_\beta^\kappa$ | × 5 | LHA, width, thrust, multiplicity, $(p_T^D)^2$ |
| Jet $p_T$ | | $50 < p_T < 65\,\text{GeV}, \ldots, p_T > 1000\,\text{GeV}$ |
| Jet radius parameter $R$ | × 2 | 0.4 vs. 0.8 |
| Constituents | × 2 | Charged+neutral vs. charged |
| Grooming | × 2 | Ungroomed vs. groomed |

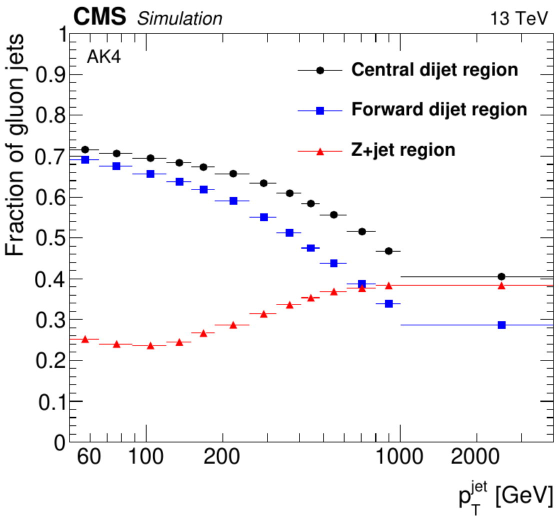


**generalized angularities**
weighted sums of jet constituents by momentum fraction $z$ and angular distance $\Delta R$ to jet axis

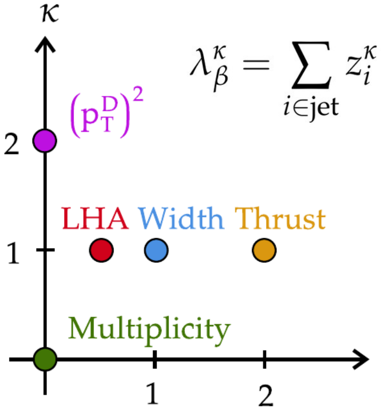


$$\lambda_\beta^\kappa = \sum_{i\in\text{jet}} z_i^\kappa \left(\frac{\Delta R_i}{R}\right)^\beta$$

**only charged constituents**
benefit from increased tracking resolution

**groomed jets:** *soft-drop* algorithm removes soft and wide-angle radiation from jets
→ more resilient to pileup, UE, ISR

# Jet substructure measurements

[4] **CMS-SMP-20-010**
arXiv:2109.03340

predictions of jet substructure observables from MC generators at NLO are compared to the measurements (5 representative configurations shown)

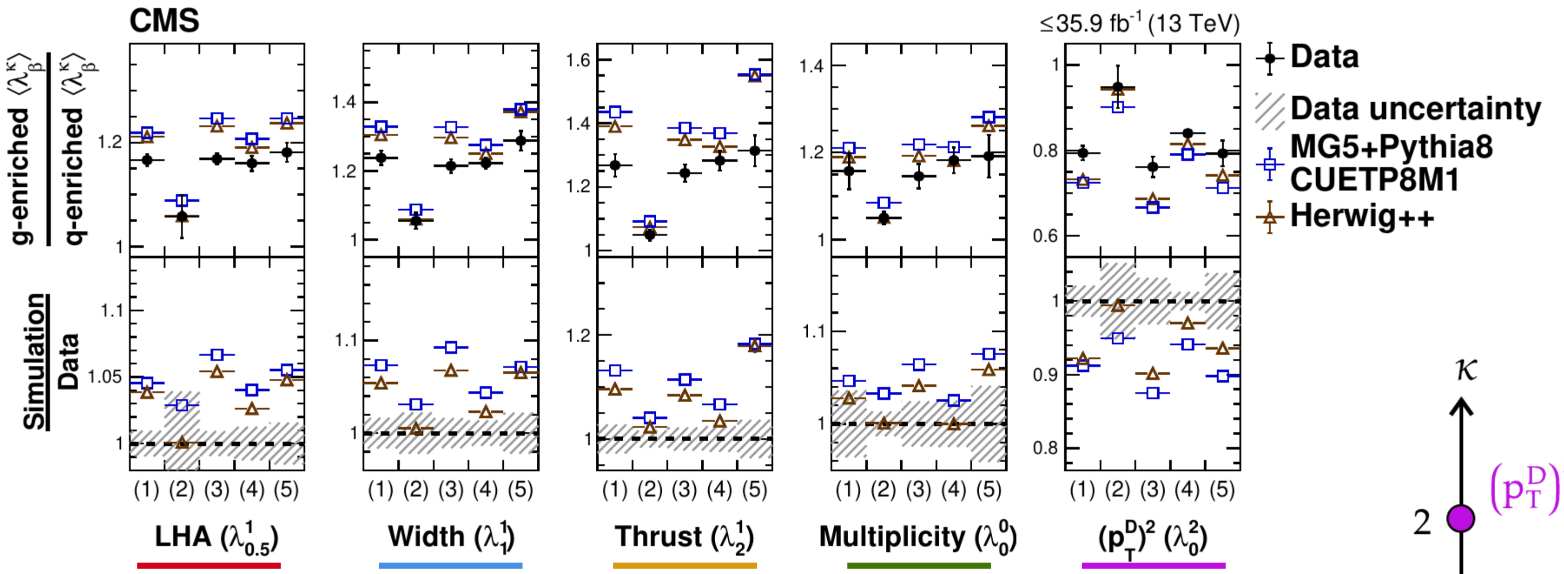


**(1) AK4, [120, 150] GeV**
**(2) AK4, [1, 4] TeV**
**(3) AK8, [120, 150] GeV**
**(4) AK4, [120, 150] GeV, charged**
**(5) AK4, [120, 150] GeV, groomed**

**IR- & collinear-safe observables**
more sensitive to perturbative emissions in jets

**not IR- & collinear-safe**
larger contributions from non-perturbative effects

$$\lambda_\beta^\kappa = \sum_{i\in \text{jet}} z_i^\kappa \left(\frac{\Delta R_i}{R}\right)^\beta$$

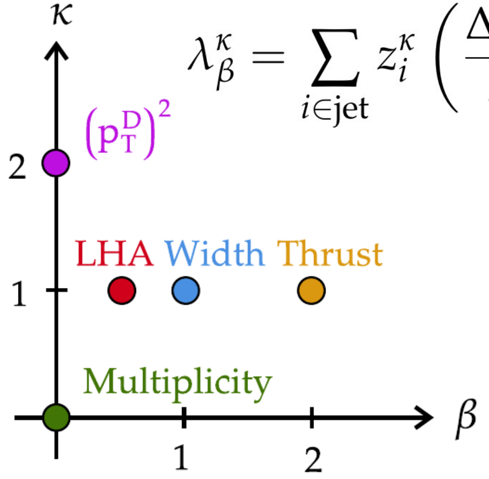


MC generators systematically overestimate ratio of $\lambda_\beta^\kappa$ in g-/q-jet samples
→ improved modeling needed to fully describe jet substructure

# **Summary** – recent jet-related results from CMS

**inclusive jet cross section** measured across a large phase space, compared to NNLO pQCD predictions

- reference results at 13 TeV for $R = 0.4$ and 0.7, complemented by $R = 0.4$ measurement at 5.02 TeV
- improved description of data by NNLO theory compared to NLO(+NLL)

**detailed QCD analyses** using latest theory predictions and tests of EFT extensions to the Standard Model

- simultaneous fit of PDFs and $\alpha_s(m_Z)$:
  - CMS jet data result in smaller uncertainties, esp. for gluon PDF at high $x$,
  - reduction in scale uncertainty on $\alpha_s(m_Z)$
- inclusive jet data provide additional constraints leading to improvements on top quark mass from $t\bar{t}$ data
- study of four-quark contact interactions (CI) with different coupling structures at several energy scales

**multijet observables** → jet multiplicities, $p_T$ spectra of first four $p_T$-leading jets

- comparison of parton branching (PB) parton shower model with transverse-momentum-dependent PDFs (TMDs) to conventional parton shower models with collinear PDFs → similar description of data

extensive investigation of **jet substructure** observables in data and MC simulation at LO and NLO

- MC modeling of substructure still in need of improvement

*Thank you for your attention!*

# References


[1] CMS Collaboration, *"Measurement and QCD analysis of double-differential inclusive jet cross sections in pp collisions at $\sqrt{s}$ = 13 TeV"*, 2021, arXiv:2111.10431, CMS-SMP-20-011, CERN-EP-2021-221, http://cds.cern.ch/record/2791017, INSPIRE ID 1972986. Accepted by *JHEP*. All figures and tables can be found at http://cms-results.web.cern.ch/cms-results/public-results/publications/SMP-20-011 (CMS Public Pages);

[2] CMS Collaboration, *"Measurement of the double-differential inclusive jet cross section in proton-proton collisions at $\sqrt{s}$ = 5.02 TeV"*, 2021, CMS-PAS-SMP-21-009, http://cds.cern.ch/record/2777126. INSPIRE ID 1920674;

[3] CMS Collaboration, *"Cross section measurements of jet multiplicity and jet transverse momenta in multijet events at $\sqrt{s}$ = 13 TeV"*, 2021, CMS-PAS-SMP-21-006, http://cds.cern.ch/record/2776772. INSPIRE ID 1920696;

[4] CMS Collaboration, *"Study of quark and gluon jet substructure in Z+jet and dijet events from pp collisions"*, 2021, arXiv:2109.03340, CMS-SMP-20-010, CERN-EP-2021-161, http://cds.cern.ch/record/2780472, INSPIRE ID 1920187. Accepted by *JHEP*. All figures and tables can be found at http://cms-results.web.cern.ch/cms-results/public-results/publications/SMP-20-010 (CMS Public Pages);

[5] F. Hautmann et al., *"Collinear and TMD quark and gluon densities from parton branching solution of QCD Evolution Equations"*, *JHEP* **01** (2018) 070, doi:10.1007/JHEP01(2018)070, arXiv:1708.03279;

[6] A. Bermudez Martinez et al., *"Collinear and TMD parton densities from fits to precision DIS measurements in the parton branching method"*, *Phys. Rev. D* **99** (2019), no. 7, 074008, doi:10.1103/PhysRevD.99.074008, arXiv:1804.11152

# Backup

# Inclusive jet production at $\sqrt{s}$ = 13 TeV

[1] **CMS-SMP-20-011**
arXiv:2111.10431

double-differential cross section in jet $p_T$ and rapidity $y$

*shown here*: anti-$k_T$ jets with $R = 0.4$

comparison to pQCD theory at NLO+NLL and NNLO,
+ non-perturbative (NP) and electroweak (EW) corrections

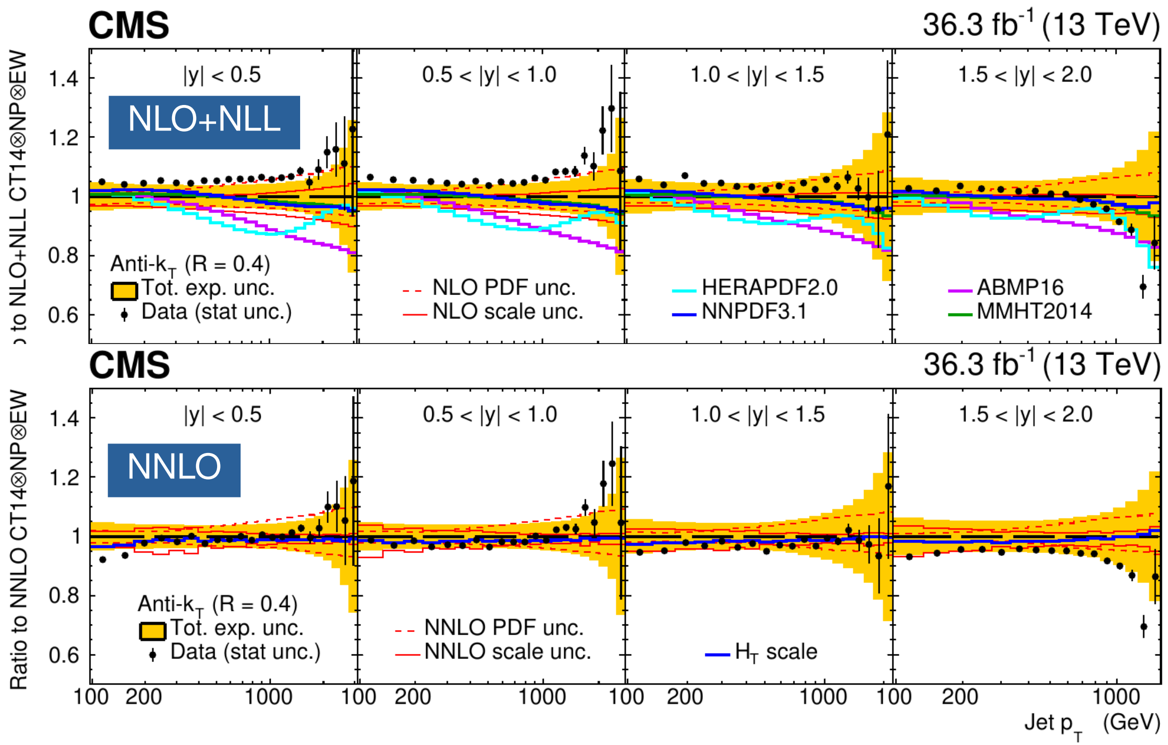


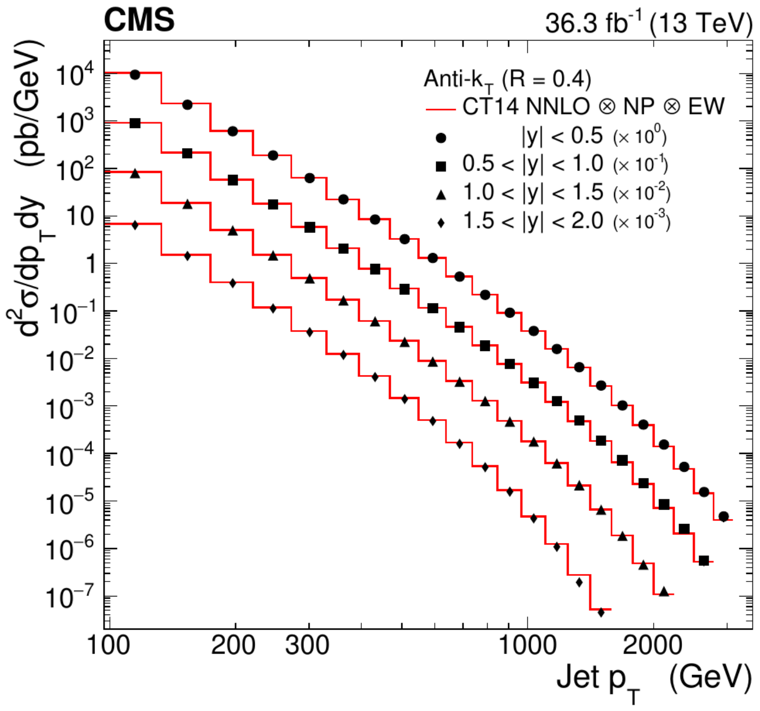

# Non-perturbative and electroweak corrections

corrections for non-perturbative (NP) effects: hadronization, multi-parton interactions (MPI)

derived from particle-level MC simulations

effect size depends strongly on jet radius

electroweak (EW) corrections

largest at high $p_T$ at central rapidities

little dependence on jet radius

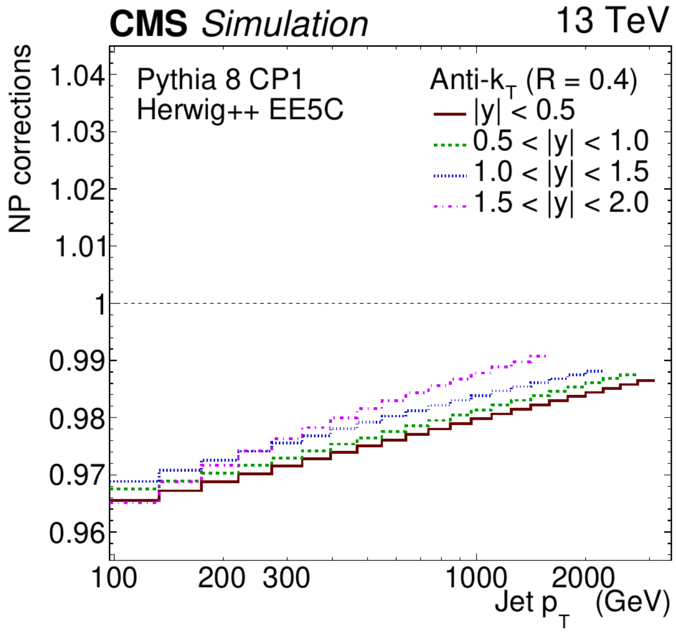


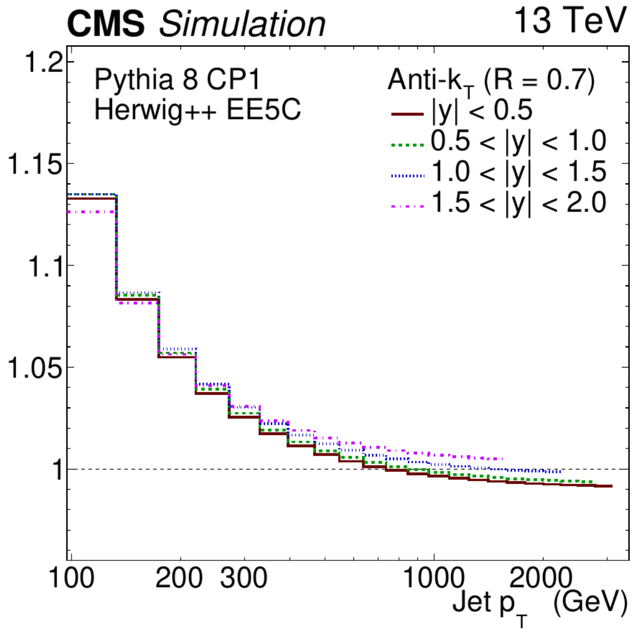


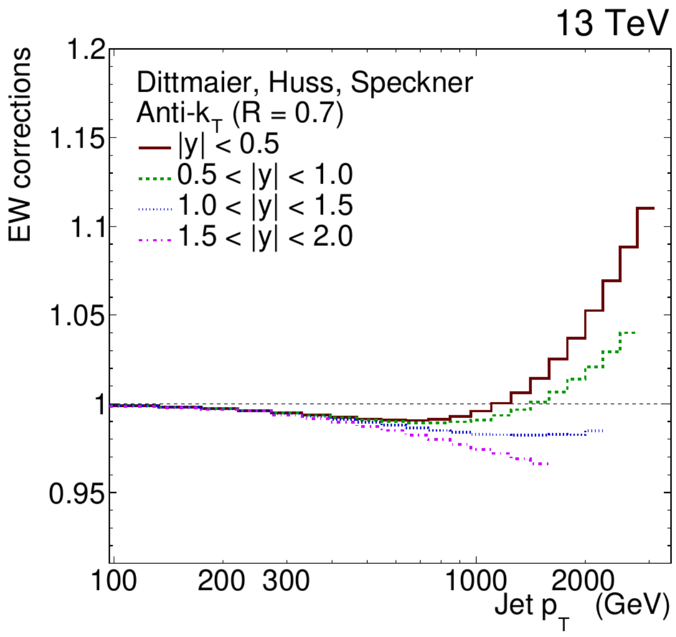

# Inclusive jets at $\sqrt{s}$ = 13 TeV – unfolding

full 2D unfolding across jet $p_T$ and $|y|$

response matrix depicts event migrations between the particle and detector levels

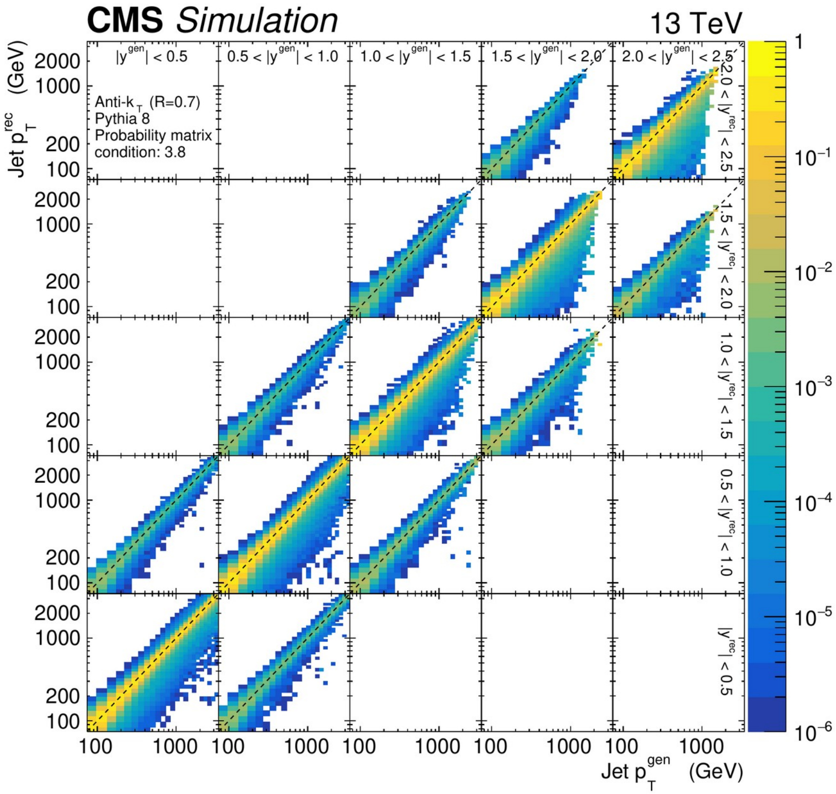


statistical correlations on particle-level spectra induced by the unfolding procedure

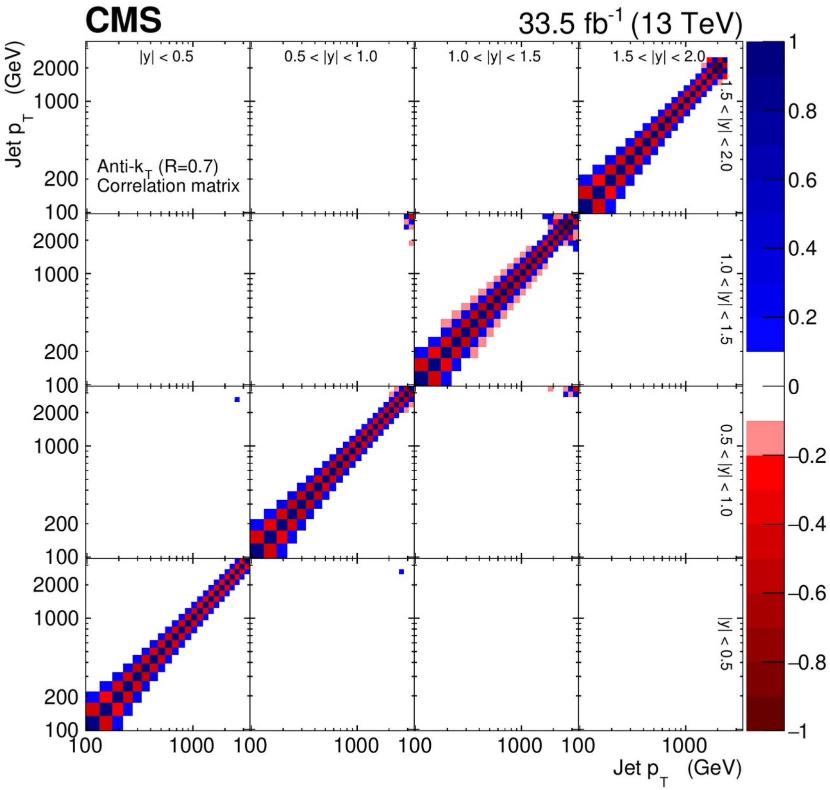

# Inclusive jet production at $\sqrt{s}$ = 13 TeV

[1] **CMS-SMP-20-011**
arXiv:2111.10431

## profiling analysis of **PDFs**

evaluate impact of new data with CT14 PDFs as a starting point

- theory at NLO and NNLO
- inclusive jet and $t\bar{t}$ data

overall reduction of PDF uncertainty
inclusion of $t\bar{t}$ data beneficial at high $x$

## profiling analysis of $\alpha_s(m_Z)$

strong coupling constant is varied consistently with $\alpha_s$ series PDFs

slightly lower $\alpha_s(m_Z)$ value at NNLO

uncertainty due to missing higher orders (scale uncertainty) is reduced

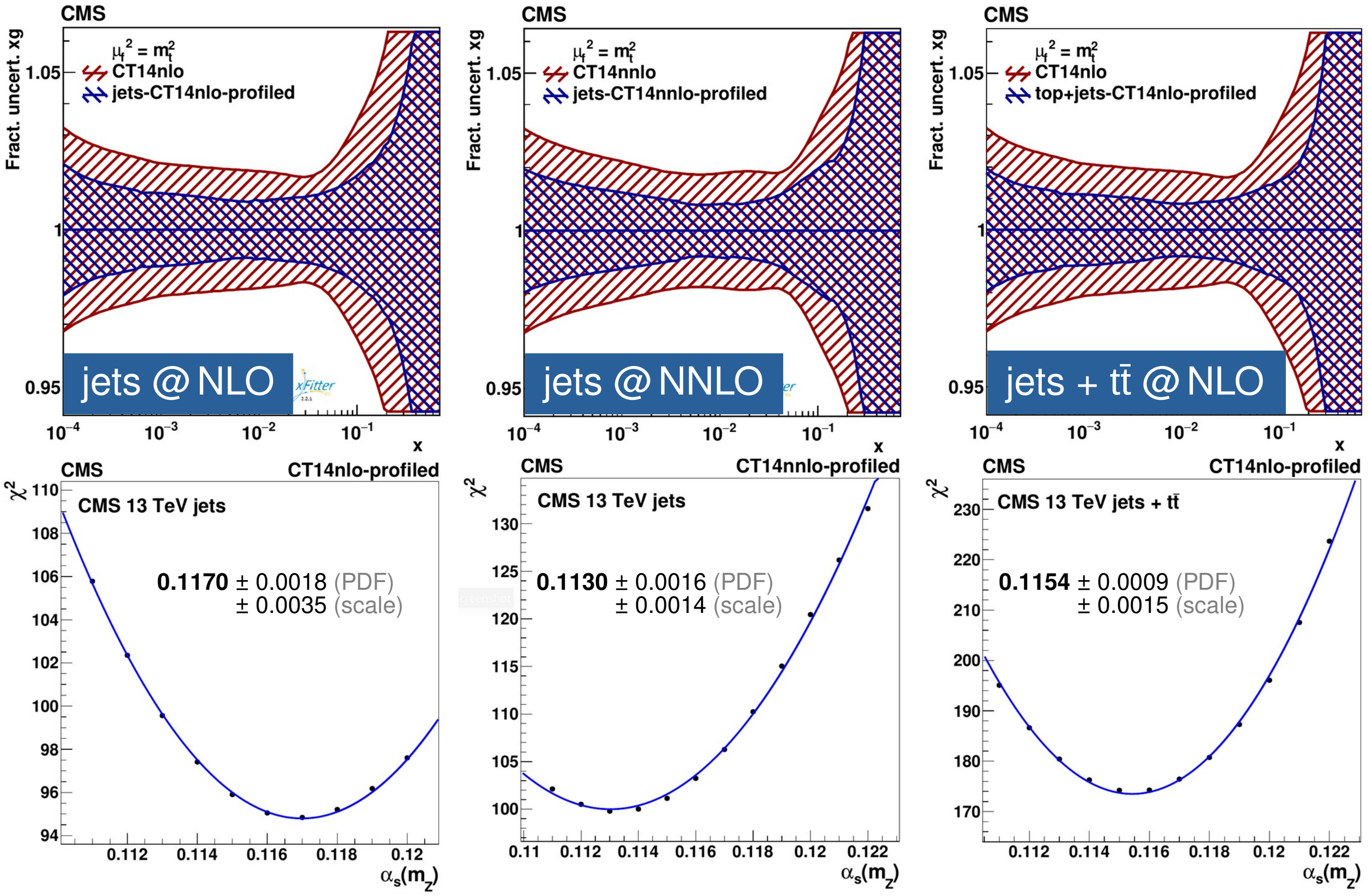

# **PDF profiling** – impact of CMS jet data at NLO & NNLO

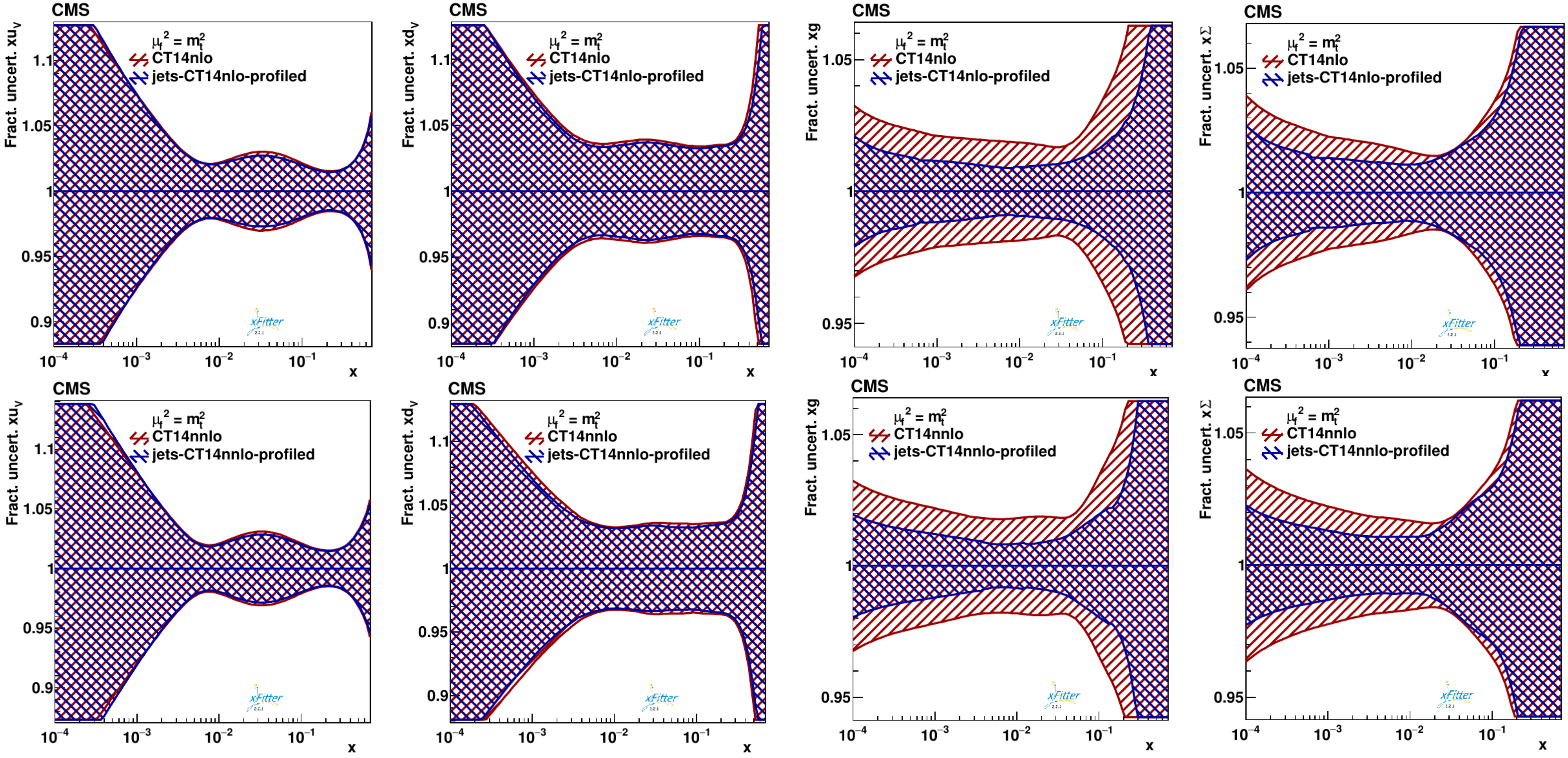

# **Full PDF fit** – impact of CMS jet data & uncertainties

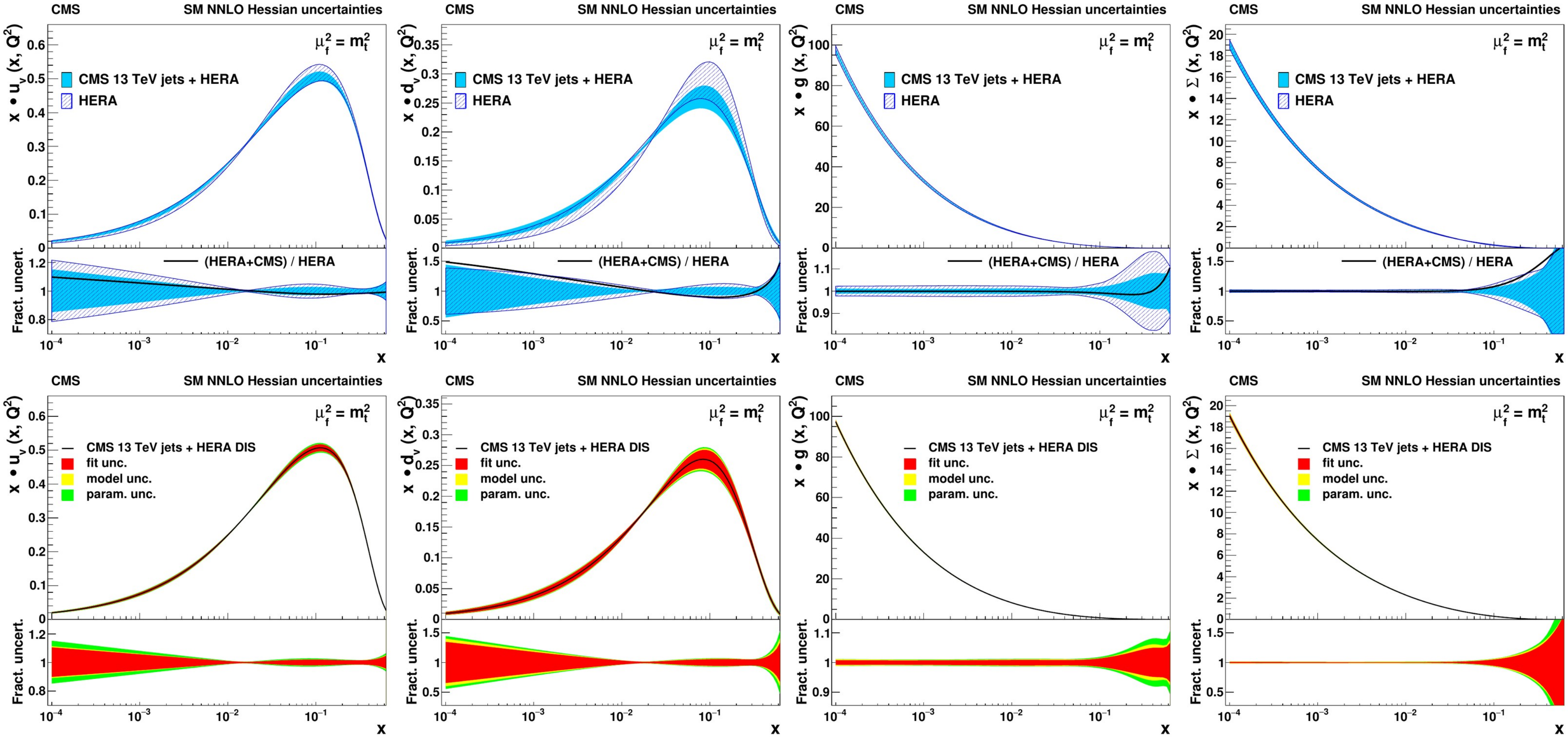

# **Full PDF fit** – inclusion of $t\bar{t}$ data & SMEFT fit

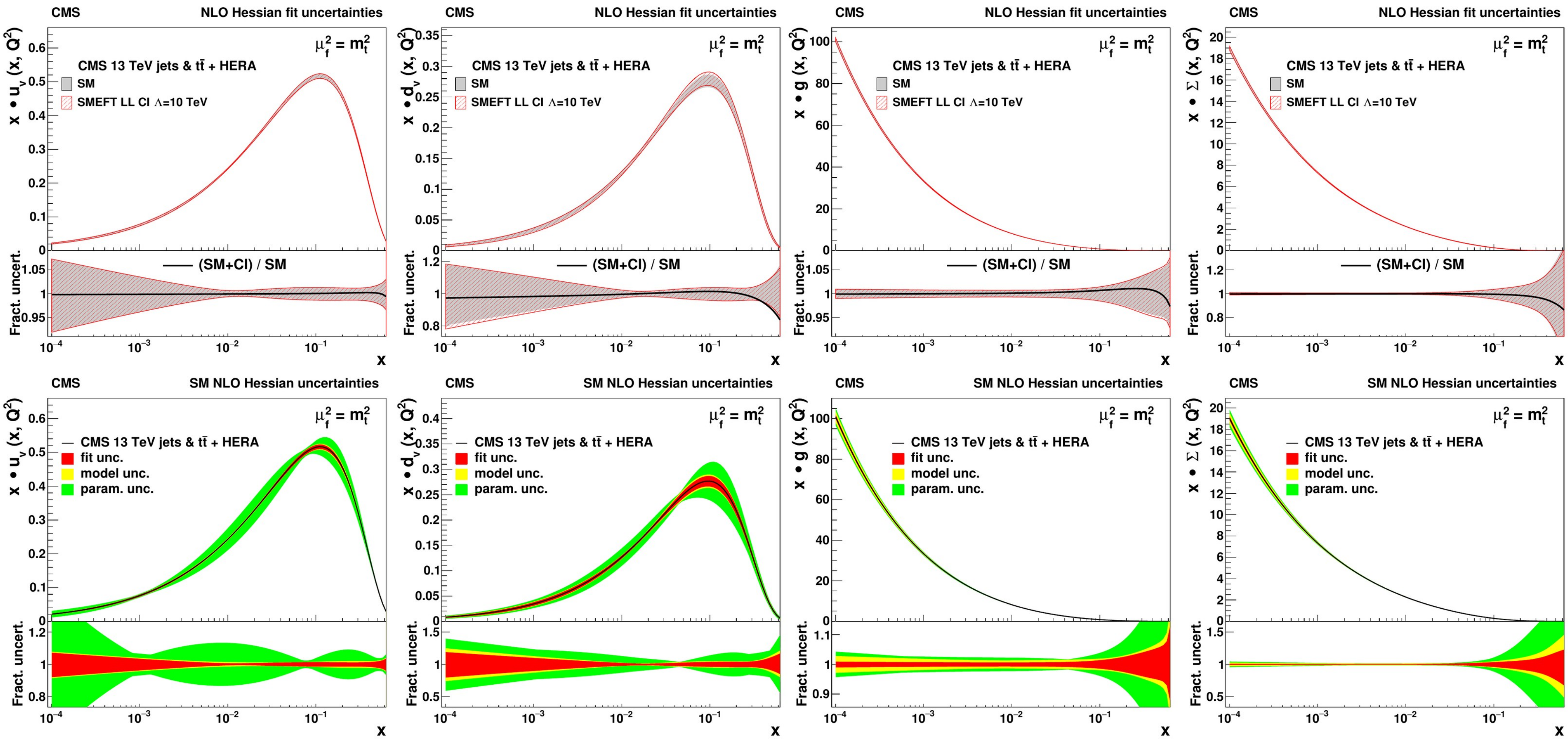

# **CI model fit** – energy scales and Wilson coefficients

Table 7: The values and uncertainties of the fitted Wilson coefficients $c_1$ for various scales $\Lambda$. The fit uncertainties are obtained by using the Hessian method.

| Scale | CI model | $c_1$ | Fit | Model | Scale | Param. |
|---|---|---|---|---|---|---|
| | Left-handed | $-0.017$ | 0.0047 | 0.0001 | 0.004 | 0.002 |
| $\Lambda = 5$ TeV | Vector-like | $-0.009$ | 0.0026 | 0.0001 | 0.002 | 0.001 |
| | Axial vector-like | $-0.009$ | 0.0025 | 0.0001 | 0.002 | 0.001 |
| | Left-handed | $-0.068$ | 0.019 | 0.003 | 0.016 | 0.009 |
| $\Lambda = 10$ TeV | Vector-like | $-0.037$ | 0.011 | 0.002 | 0.008 | 0.006 |
| | Axial vector-like | $-0.036$ | 0.011 | 0.003 | 0.008 | 0.005 |
| | Left-handed | $-0.116$ | 0.033 | 0.006 | 0.026 | 0.015 |
| $\Lambda = 13$ TeV | Vector-like | $-0.063$ | 0.018 | 0.004 | 0.015 | 0.008 |
| | Axial vector-like | $-0.062$ | 0.018 | 0.003 | 0.014 | 0.008 |
| | Left-handed | $-0.28$ | 0.08 | 0.01 | 0.06 | 0.04 |
| $\Lambda = 20$ TeV | Vector-like | $-0.15$ | 0.04 | 0.01 | 0.04 | 0.02 |
| | Axial vector-like | $-0.15$ | 0.04 | 0.01 | 0.04 | 0.02 |
| | Left-handed | $-1.8$ | 0.53 | 0.08 | 0.42 | 0.23 |
| $\Lambda = 50$ TeV | Vector-like | $-1.0$ | 0.28 | 0.05 | 0.23 | 0.13 |
| | Axial vector-like | $-1.0$ | 0.29 | 0.04 | 0.23 | 0.13 |

# Inclusive jets $\sqrt{s}$ = 5.02 TeV – comparison to NLO theory

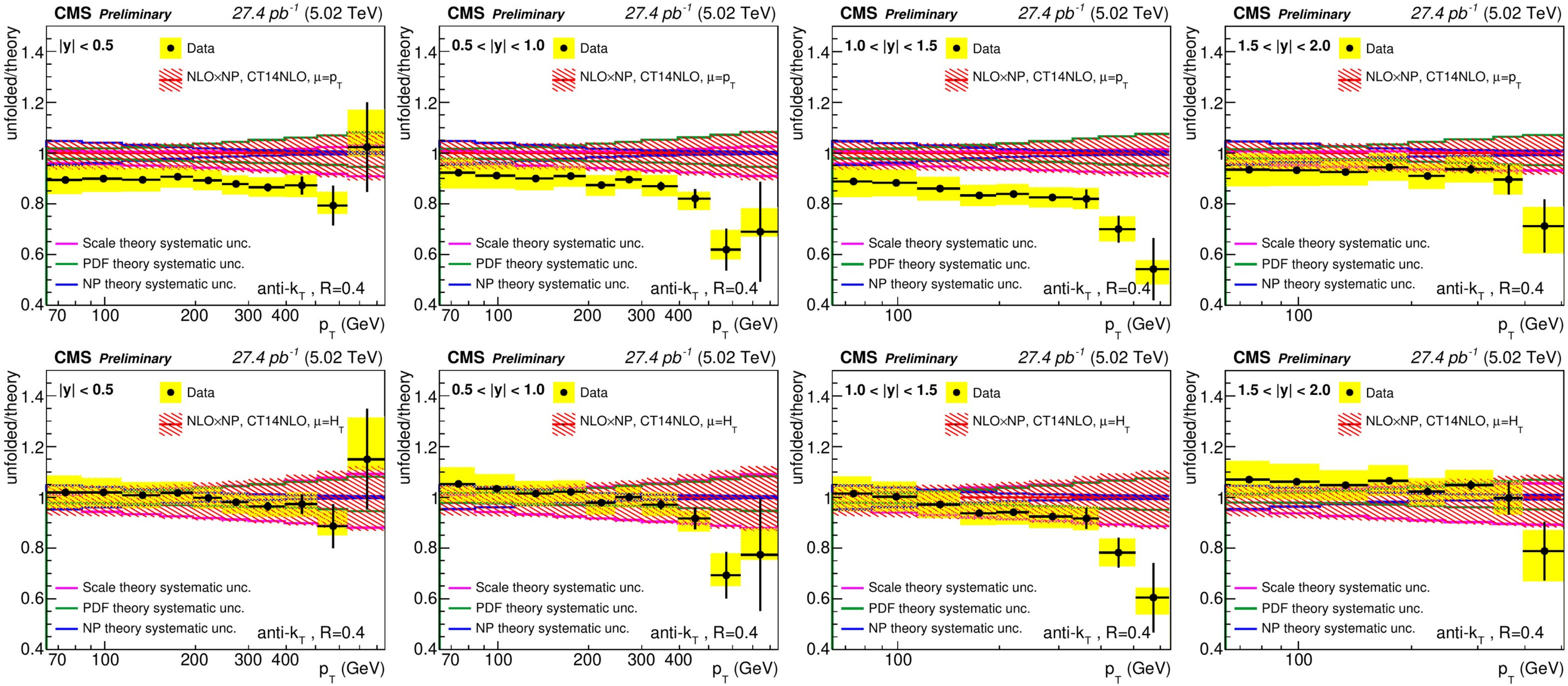

# Inclusive jets $\sqrt{s}$ = 5.02 TeV – comparison to NNLO theory

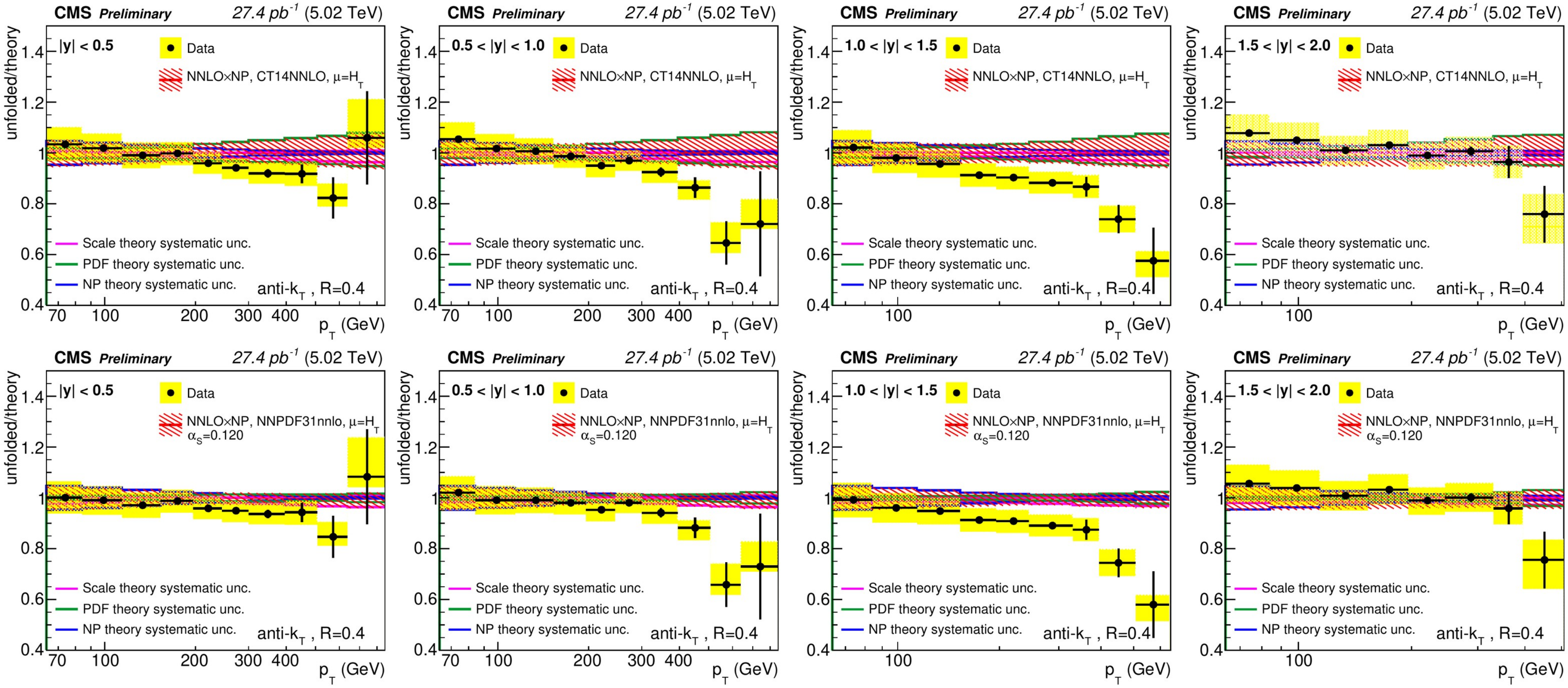

# Inclusive jets $\sqrt{s}$ = 5.02 TeV – sensitivity to $\alpha_s(m_Z)$

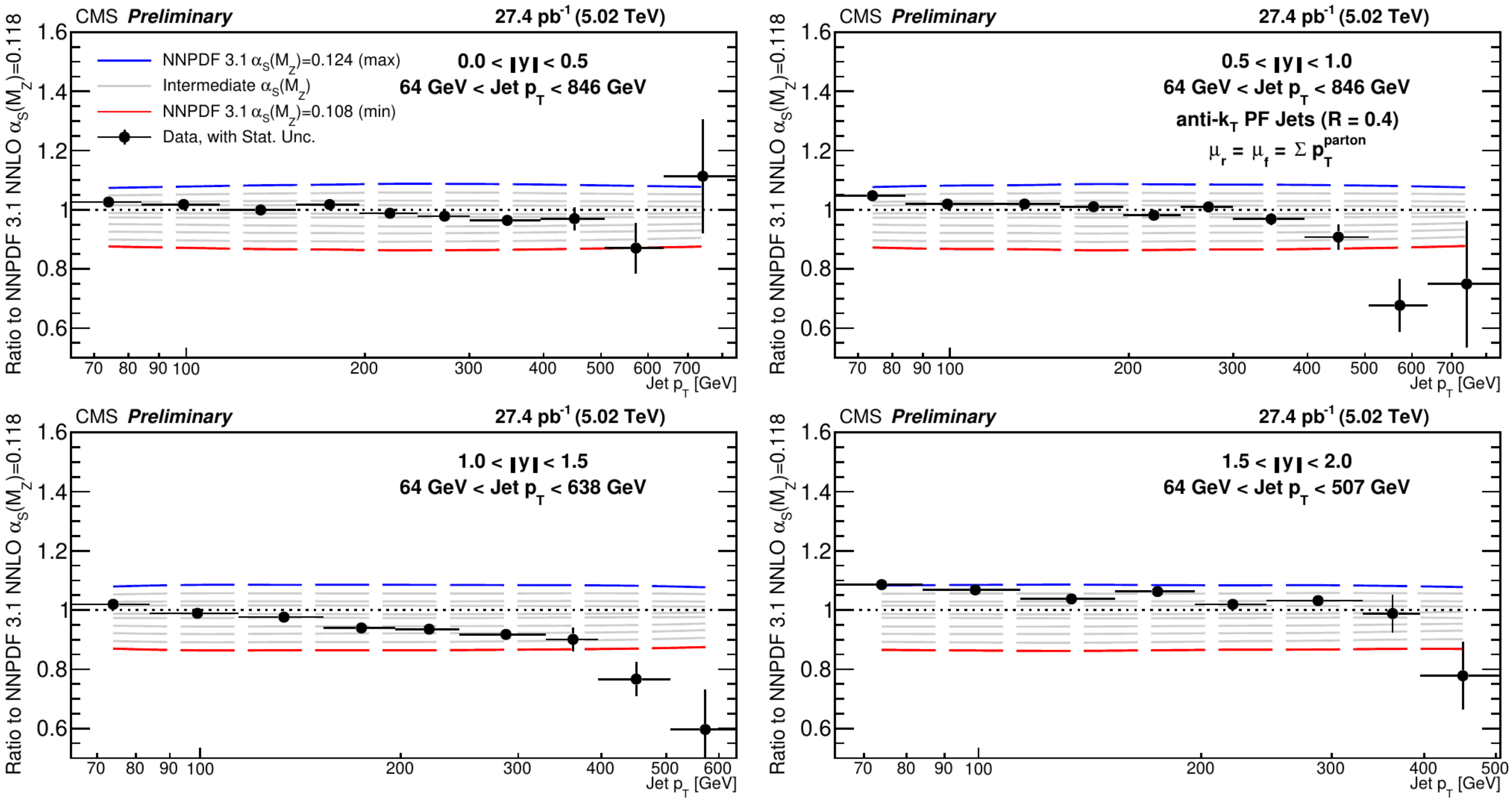

# Multijet measurements – jet $p_T$ spectra at LO & NLO

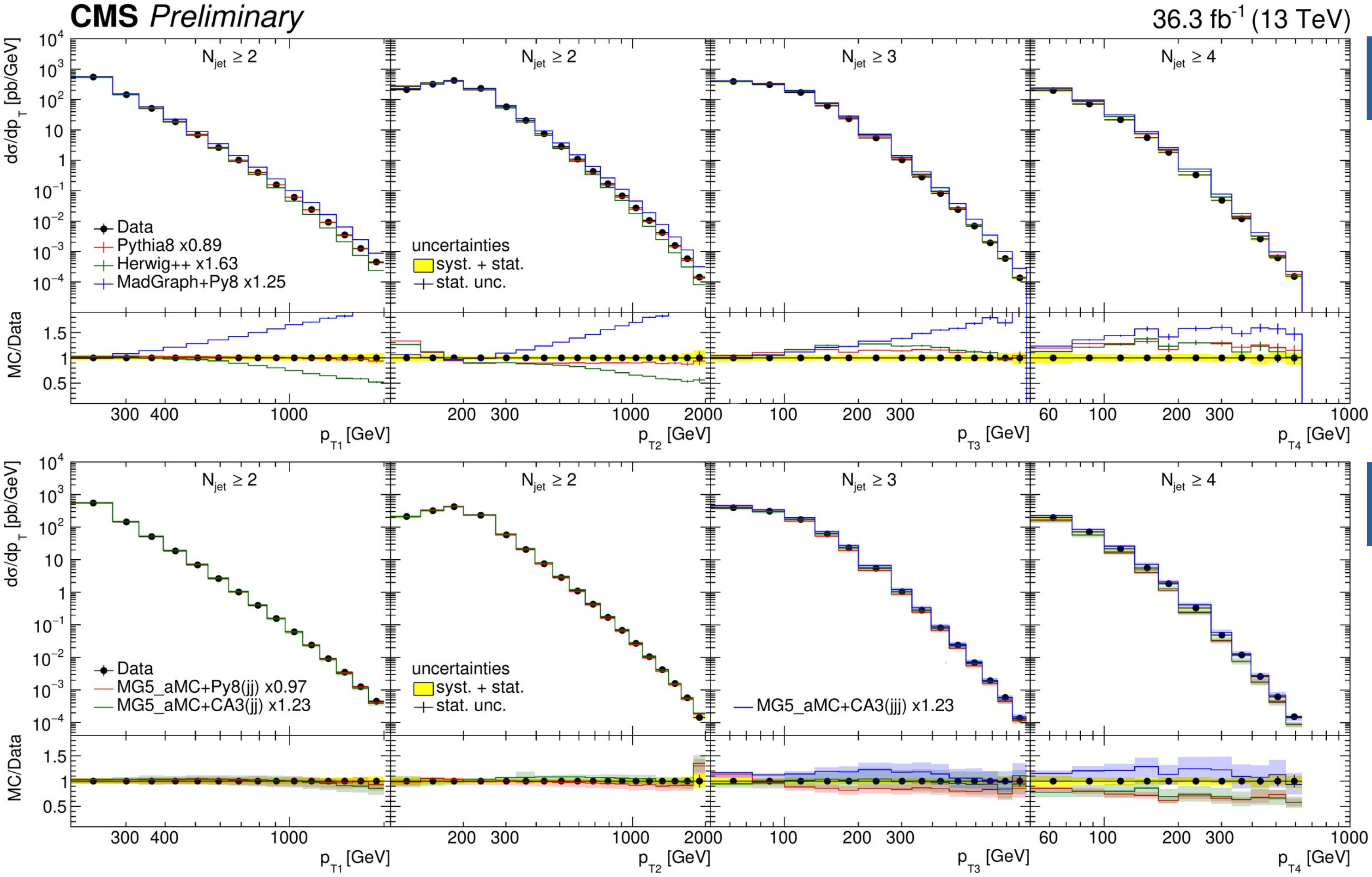


LO models

[3] **CMS-SMP-21-006**

| generator | PDF |
|---|---|
| PYTHIA 8 | NNPDF 2.3 (LO) |
| MADGRAPH+PY8 | NNPDF 2.3 (LO) |
| HERWIG++ | CTEQ6L1 (LO) |

NLO models

| | |
|---|---|
| MG5_AMC+PY8 (*jj*) | NNPDF 3.0 (NLO) |
| MG5_AMC+CA3 (*jj*) | PB set 2 (NLO) |
| MG5_AMC+CA3 (*jjj*) | PB set 2 (NLO) |

# Multijet measurements – jet multiplicities (lower $p_T$ range)

[3] **CMS-SMP-21-006**

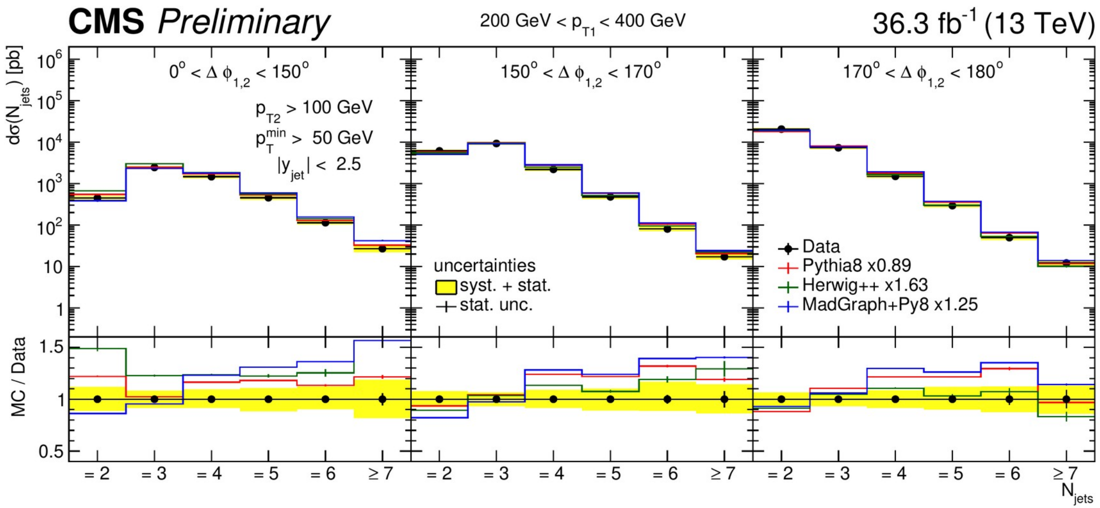


LO models

| | generator | PDF | matrix element | tune |
|---|---|---|---|---|
| red | PYTHIA 8 | NNPDF 2.3 (LO) | LO $2 \rightarrow 2$ | CUETP8M1 |
| blue | MADGRAPH+PY8 | NNPDF 2.3 (LO) | LO $2 \rightarrow 2,3,4$ | CUETP8M1 |
| green | HERWIG++ | CTEQ6L1 (LO) | LO $2 \rightarrow 2$ | CUETHppS1 |

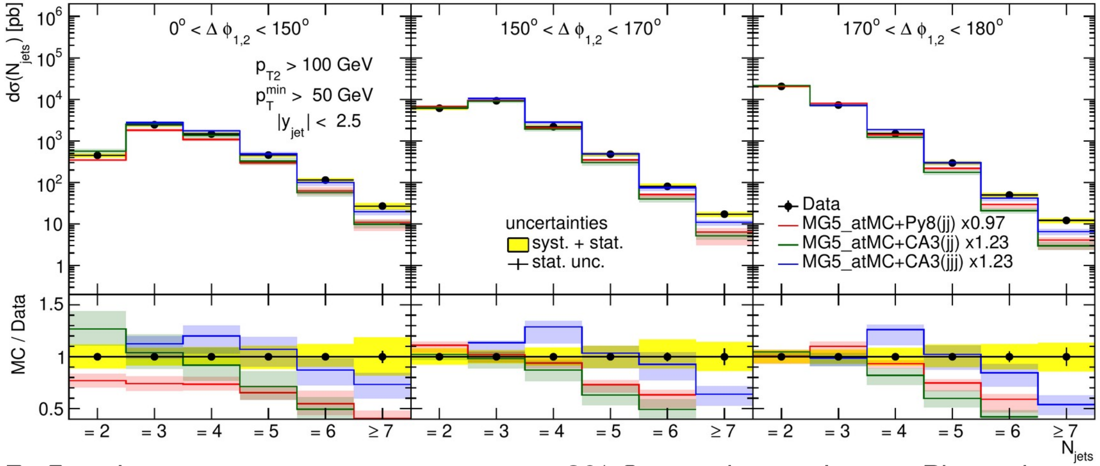


NLO models

| | generator | PDF | matrix element | tune |
|---|---|---|---|---|
| red | MG5_AMC+PY8 $(jj)$ | NNPDF 3.0 (NLO) | NLO $2 \rightarrow 2$ | CUETP8M1 |
| green | MG5_AMC+CA3 $(jj)$ | PB set 2 (NLO) | NLO $2 \rightarrow 2$ | – |
| blue | MG5_AMC+CA3 $(jjj)$ | PB set 2 (NLO) | NLO $2 \rightarrow 3$ | – |

# Multijet measurements – jet multiplicities (medium $p_T$ range)

[3] **CMS-SMP-21-006**

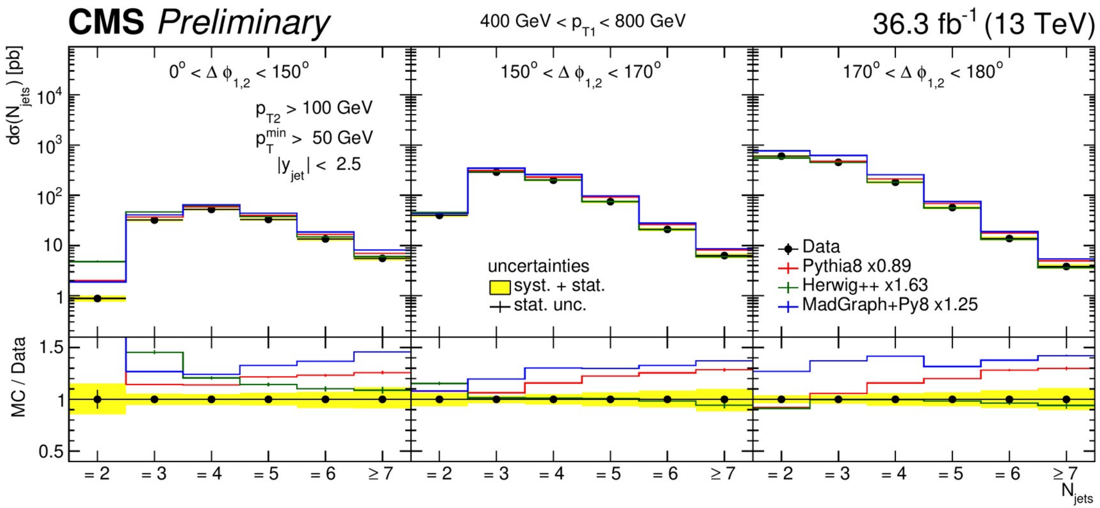


LO models

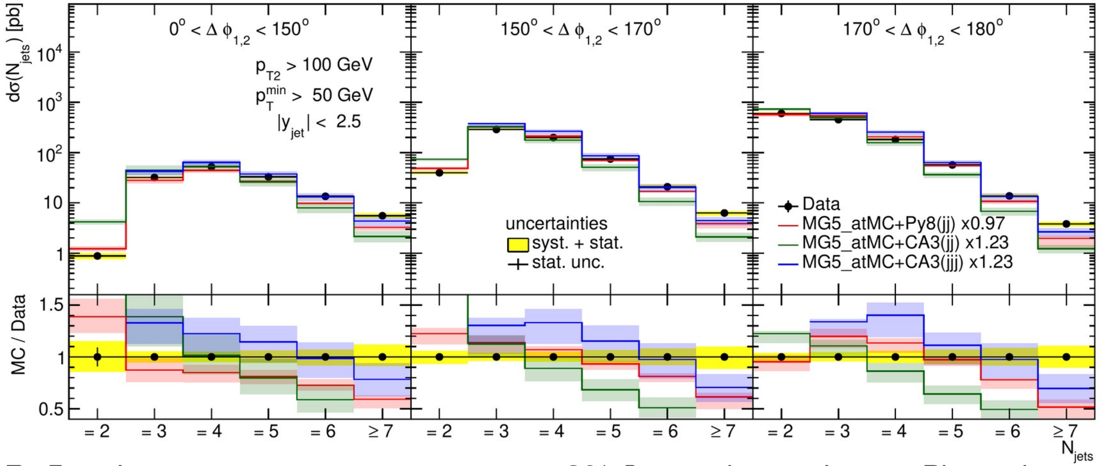


NLO models

| generator | PDF | matrix element | tune |
|---|---|---|---|
| PYTHIA 8 | NNPDF 2.3 (LO) | LO $2 \to 2$ | CUETP8M1 |
| MADGRAPH+PY8 | NNPDF 2.3 (LO) | LO $2 \to 2,3,4$ | CUETP8M1 |
| HERWIG++ | CTEQ6L1 (LO) | LO $2 \to 2$ | CUETHppS1 |
| MG5_AMC+PY8 (*jj*) | NNPDF 3.0 (NLO) | NLO $2 \to 2$ | CUETP8M1 |
| MG5_AMC+CA3 (*jj*) | PB set 2 (NLO) | NLO $2 \to 2$ | – |
| MG5_AMC+CA3 (*jjj*) | PB set 2 (NLO) | NLO $2 \to 3$ | – |

# Multijet measurements – jet multiplicities (higher $p_T$ range)

[3] **CMS-SMP-21-006**

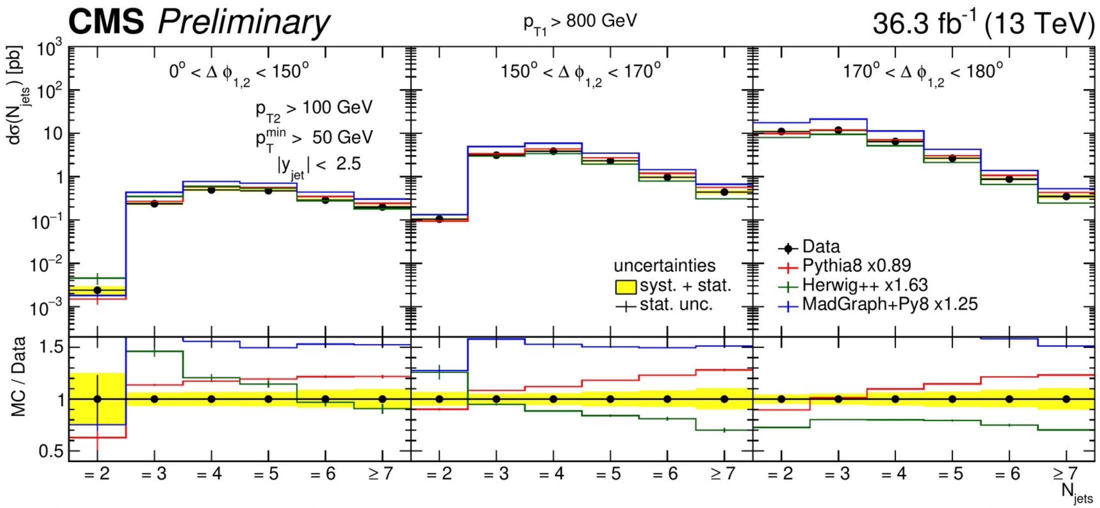


LO models

| generator | PDF | matrix element | tune |
|---|---|---|---|
| PYTHIA 8 | NNPDF 2.3 (LO) | LO $2 \to 2$ | CUETP8M1 |
| MADGRAPH+PY8 | NNPDF 2.3 (LO) | LO $2 \to 2,3,4$ | CUETP8M1 |
| HERWIG++ | CTEQ6L1 (LO) | LO $2 \to 2$ | CUETHppS1 |

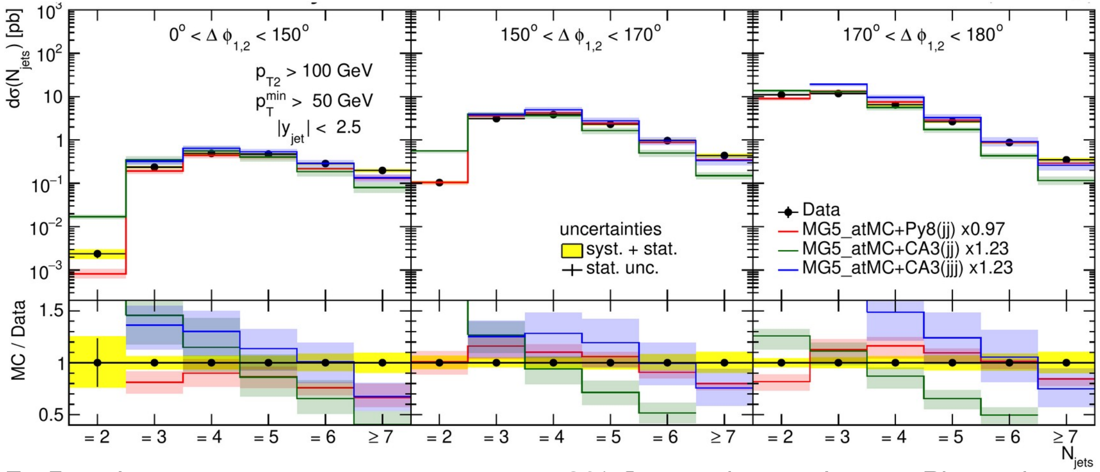


NLO models

| | | | |
|---|---|---|---|
| MG5_AMC+PY8 ($jj$) | NNPDF 3.0 (NLO) | NLO $2 \to 2$ | CUETP8M1 |
| MG5_AMC+CA3 ($jj$) | PB set 2 (NLO) | NLO $2 \to 2$ | – |
| MG5_AMC+CA3 ($jjj$) | PB set 2 (NLO) | NLO $2 \to 3$ | – |